

UCRL- 92974  
PREPRINT

**CIRCULATION COPY  
SUBJECT TO RECALL  
IN TWO WEEKS**

CONDENSED MATTER AT HIGH SHOCK PRESSURES

W. J. Nellis  
N. C. Holmes  
A. C. Mitchell  
H. B. Radousky  
D. Hamilton

This paper was prepared for submittal to  
Fifteenth International Symposium on  
Shock Waves and Shock Tubes  
Lawrence Berkeley Laboratory  
July 29-August 1, 1985  
Berkeley, CA  
July 12, 1985



Lawrence  
Livermore  
National  
Laboratory

This is a preprint of a paper intended for publication in a journal or proceedings. Since changes may be made before publication, this preprint is made available with the understanding that it will not be cited or reproduced without the permission of the author.



## DISCLAIMER

This document was prepared as an account of work sponsored by an agency of the United States Government. Neither the United States Government nor the University of California nor any of their employees, makes any warranty, express or implied, or assumes any legal liability or responsibility for the accuracy, completeness, or usefulness of any information, apparatus, product, or process disclosed, or represents that its use would not infringe privately owned rights. Reference herein to any specific commercial products, process, or service by trade name, trademark, manufacturer, or otherwise, does not necessarily constitute or imply its endorsement, recommendation, or favoring by the United States Government or the University of California. The views and opinions of authors expressed herein do not necessarily state or reflect those of the United States Government or the University of California, and shall not be used for advertising or product endorsement purposes.

# CONDENSED MATTER AT HIGH SHOCK PRESSURES

W. J. Nellis, N. C. Holmes, A. C. Mitchell, H. B. Radousky, and D. Hamilton

Lawrence Livermore National Laboratory  
University of California  
Livermore, California 94550

Experimental techniques are described for shock waves in liquids: Hugoniot equation-of-state, shock temperature and emission spectroscopy, electrical conductivity, and Raman spectroscopy. Experimental data are reviewed and presented in terms of phenomena that occur at high densities and temperatures in shocked He, Ar, N<sub>2</sub>, CO, SiO<sub>2</sub>-aerogel, H<sub>2</sub>O, and C<sub>6</sub>H<sub>6</sub>. The superconducting properties of Nb metal shocked to 100 GPa (1 Mbar) and recovered intact are discussed in terms of prospects for synthesizing novel, metastable materials. Ultrahigh pressure data for Cu is reviewed in the range 0.3-6 TPa (3-60 Mbar).

## I. INTRODUCTION

Significant advances in shocked, condensed matter have been made in recent years through diagnostic development, specimen fabrication, and theory. The nature of this work is summarized in the proceedings of recent Topical Conferences on Shock Waves in Condensed Matter.<sup>1,2</sup> General areas of concentration have been the properties of fluids and solids at high densities, temperatures, and strain rates and the nature of materials processed and recovered from high dynamic pressures. In this paper the main emphasis will be on dense fluids at shock pressures up to 100 GPa (1 Mbar), compressions up to 5-fold over initial liquid density, and shock temperatures up to 10,000K. At such extreme conditions several phenomena occur including molecular repulsion, rotation, vibration, and dissociation, electronic and molecular ionization, and chemical decomposition and reaction. Examples from the literature will be reviewed and new results will be presented to illustrate these phenomena.

The properties of dense molecular fluids at high pressures and temperatures have three principal applications: the equation of state and chemistry of high explosives, the nature of the interiors of the outer planets (Jupiter, Saturn, Uranus, and Neptune), and hydrodynamic applications. The relation between these areas and shock-compression studies was discussed previously.<sup>3</sup>

## II. EXPERIMENTS

The experiments are performed using shock waves generated by the impact of planar projectiles onto planar target specimens. While, historically, strong shock waves have been generated using high explosives,<sup>4</sup> in recent years most research has utilized impactors launched by light-gas guns.<sup>5</sup> Maximum impact velocities are 2 and 8 km/s for single-stage and two-stage light-gas guns, respectively. A Ta impactor at 2 and 8 km/s achieves shock pressures in Al of 30 and 200 GPa, respectively. Gas guns have several advantages over explosive shock generators. Shock strength is simply tuneable by choice of impactor material and velocity, shock-wave profile is simply tuneable by choice of impactor thickness and design, shock pressures twice as large as with plane wave explosive systems are available, and facilities are operated in a conventional laboratory setting. The current state of temporal

and spatial resolution for shock-wave diagnostics means that gun facilities can now be scaled down substantially without compromising the ability to perform novel and diverse research with a well characterized and simply tuneable shock driver.

The experiments discussed here were performed using a two-stage light-gas gun described previously.<sup>6-8</sup> The two driving media or stages are gunpowder reaction products and H<sub>2</sub> gas. The gunpowder drives a heavy piston which compresses the H<sub>2</sub> gas. When the H<sub>2</sub> pressure reaches  $\sim 100$  MPa (1 kbar) a rupture valve opens and the compressed gas accelerates a light ( $\sim 15$ g) projectile to velocities up to 8 km/s along a smooth bore launch tube. Strong shock waves are generated by impact of projectile onto target positioned about 0.5m beyond the muzzle of the launch tube. Projectile velocity is measured in free flight between muzzle and target by a flash radiograph system. A more detailed description of two-stage gun operation and shock-wave diagnostics is available.<sup>9</sup>

The fundamental measurement is equation of state which determines the pressure, density, and specific internal energy achieved in shock compression experiments. These experiments are based on the Rankine-Hugoniot relations and shock impedance matching.<sup>9</sup> The measured quantities are impactor velocity, shock velocity, and initial density. The method is described elsewhere for single- and double-shocked liquids.<sup>10,11</sup> Having measured the equation of state, other properties can be measured to study the nature of the state; for example, shock temperature, electrical conductivity, and Raman spectra. In these experiments the impactor velocity is also measured and the state achieved is obtained by shock impedance matching using the previously determined equations of state. Figures 1a and 1b illustrate experimental configurations for single and double-shock Hugoniot experiments. In the former, shock velocity is measured in the liquid, and in the latter it is measured in an anvil behind the liquid.

A shock temperature or emission spectrum measurement in a transparent liquid is illustrated in Fig. 1c. Radiation emitted from the shock front exits the unshocked portion of the specimen and is directed to either a 6-channel time-resolved pyrometer<sup>12,13</sup> or to a spectrograph and 1000-channel, time-integrated, gated, linear diode array.<sup>14</sup> For simple dense fluids like Ar, both molecular dynamics and continuum mechanics calculations indicate that the shock front is about 10 Å and  $< 10^{-12}$ s thick.<sup>15,16</sup> Thus, for simple shocked fluids the emission spectra are fit to graybody or blackbody spectra and the assumption is made that the temperature so derived is characteristic of equilibrated shocked material emitting light from behind the shock front through an optically thin shock front. For more complex fluids, for example those undergoing chemical reactions, the shock front can be optically thick, so that the equilibrium temperature is not observed while nonequilibrium spectral features might be.

A two-probe electrical conductivity experiment for a shocked liquid is illustrated in Fig. 1d.<sup>17</sup> A current is established in the shunt resistor, and the time-resolved voltage across the electrodes in parallel with the shunt resistor is measured as the shock transits the electrodes. The cell resistance versus known electrical conductivities is calibrated in separate experiments prior to the shock experiment.

The microscopic nature of shocked fluids can be investigated by pulsed Raman spectroscopy, which measures the distribution of molecular vibrational frequencies. The experimental arrangement is illustrated in Fig. 2. Light from a 10 ns 0.2J KrF (284 nm) laser pulse is incident normally on a specimen of shocked liquid. Light from spontaneous Raman scattering,  $10^{-10}$ J total, is viewed at 45° off axis, dispersed by a spectrograph, and recorded on a gated, linear diode array.<sup>18</sup> The laser light is focussed several mm behind the shock front and so this technique requires that the shocked specimen remain transparent.

In the case of transparent, brittle, solid specimens, like silica aerogel, the configuration for an equation-of-state experiment in which shock velocity is measured is shown in Fig. 3.<sup>19</sup> Because the shock front radiates strongly in the visible, the stepped rear surface is coated with  $\sim 1000 \text{ \AA}$  of Au to absorb thermal radiation until shock breakout at the coated surface. By temporally streaking the optical emission from the coated, stepped surface, the transit time of the shock across the step height can be measured. This technique is similar to that used previously to measure transit times for laser-driven shock waves in metals.<sup>20</sup> The shock temperature is measured by using a simple, uncoated specimen disc and sending light emitted from the shock front to a pyrometer or spectrograph.

Several additional measurements are made in shocked solids, including time-resolved interface velocity measurements by optical interferometry,<sup>21,22</sup> the generation of dynamic, planar, isentropic compression waves by graded-density impactors,<sup>23</sup> the detection of phase transitions by both the measurement of longitudinal sound speeds<sup>24</sup> and shock temperatures,<sup>25</sup> and flash X-ray diffraction from crystals in the shock state.<sup>26,27</sup>

In addition to the diagnostic developments major advances have resulted from specimen fabrication. For example, in order to investigate the high-density regime of molecular fluids, higher-density liquid specimens were shocked, rather than gases. In order to liquify most small molecules at atmospheric pressures, cryogenic temperatures are required. Thus, each specimen holder was a small cryostat<sup>10,28,29</sup> - a different one for each experiment. States of high-temperature matter in expansion relative to crystal density have been studied because of the recent availability of fine-grained, transparent, porous  $\text{SiO}_2$  aerogel having  $\sim 100 \text{ \AA}$  pore size.<sup>19</sup> The fine pore size means that the material is uniform and equilibrium will be achieved much faster than the time scale of the experiments. However, this material is extremely brittle and requires vacuum holders and diamond cutting tools to achieve the required micron surface flatness. Dynamic isentropic compression is now possible because of the development of impactors with linearly varying density (shock impedance) produced by careful sedimentation of metallic powders in an epoxy-like matrix.<sup>23</sup> These examples illustrate the importance of special materials and fabrication techniques in this field.

### III. THERMAL EQUILIBRIUM

Shocked condensed matter is generally in thermal equilibrium during the measurements owing to the high densities and temperatures. For example, liquid  $\text{N}_2$  shocked to  $30 \text{ GPa}$ <sup>10</sup> has a density of  $2 \text{ g/cm}^3$  ( $4 \times 10^{22} \text{ N}_2/\text{cm}^3$ ) and a shock temperature of  $\sim 6000\text{K}$ .<sup>30</sup> Assuming the mean free path between collisions is a molecular diameter and that molecular velocity is thermal, then the intermolecular collision time is  $\sim 10^{-13}\text{s}$ . The  $\text{N}_2$  molecular vibration time is  $\sim 10^{-14}\text{s}$ . The shock front width or equilibration time in shocked dense Ar is  $\lesssim 10^{-12}\text{s}$ .<sup>16</sup> All these times are much less than the time resolutions of the diagnostic systems which are  $\sim 10^{-9}\text{s}$  and the duration of the experiments which are  $10^{-7}$ - $10^{-6}\text{s}$ . Of course, phenomena which require longer than the experimental lifetime could produce deviations from thermal equilibrium. At the conditions considered here, however, examples of nonequilibrium behavior are difficult to identify unambiguously and are most likely to occur in chemically reacting systems.

### IV. RESULTS

Equation-of-state experiments have been performed in the last few years for most small molecules including He,<sup>29</sup>  $\text{H}_2$  and  $\text{D}_2$ ,<sup>28</sup>  $\text{N}_2$ ,<sup>10,31</sup>  $\text{O}_2$ ,<sup>10</sup> air, Ar,<sup>10,32</sup> Xe,<sup>33</sup> CO,<sup>11</sup>  $\text{CH}_4$ ,<sup>11</sup>  $\text{C}_6\text{H}_6$ ,<sup>34</sup> n- $\text{C}_4\text{H}_8$  (polybutene),<sup>34</sup>

NH<sub>3</sub><sup>17</sup> and H<sub>2</sub>O.<sup>17</sup> The maximum pressures and densities, which our group has achieved in these shocked liquids, are listed in Table I. The corresponding calculated and, in some cases, measured maximum temperatures are in the range 5,000-30,000 K.

Shock temperature measurements have been performed for a number of these fluids: H<sub>2</sub>O,<sup>13</sup> NH<sub>3</sub>,<sup>35</sup> Ar,<sup>36</sup> N<sub>2</sub>,<sup>36</sup> C<sub>6</sub>H<sub>6</sub>,<sup>34</sup> and n-C<sub>4</sub>H<sub>8</sub>.<sup>34</sup> Temperature is an important thermodynamic parameter because it provides information about the distribution of internal energy between thermal and internal degrees of freedom. In the case of C<sub>6</sub>H<sub>6</sub> and possibly n-C<sub>4</sub>H<sub>8</sub> the radiating temperatures from the shock fronts are substantially lower than the temperatures calculated theoretically assuming chemical equilibrium. This difference suggests that the radiating temperatures are not representative of shocked matter in thermal and chemical equilibrium behind the shock front.<sup>34</sup>

The electrical conductivity has been measured for shocked H<sub>2</sub>O,<sup>17,37</sup> NH<sub>3</sub>,<sup>38</sup> N<sub>2</sub>,<sup>39</sup> O<sub>2</sub>,<sup>39</sup> and C<sub>6</sub>H<sub>6</sub>.<sup>39</sup> The purpose is to determine the magnitude and mechanisms of electrical conduction and in so doing to possibly obtain information about the nature of the fluids which cannot be obtained from state variables. For example, the high conductivity of shocked H<sub>2</sub>O indicates a significant amount of H<sub>2</sub>O molecules are chemically ionized above 20 GPa shock pressure.<sup>37</sup> This proposal motivated the Raman spectroscopy measurements described below in order to look for ionic species like OH<sup>-</sup> and H<sub>3</sub>O<sup>+</sup>. The electrical conductivities of shocked N<sub>2</sub> and O<sub>2</sub> are even higher than for H<sub>2</sub>O and electrons are probably the dominant conduction mechanism.

The spontaneous Raman spectra of shocked water has been measured from 7-26 GPa<sup>18</sup> to try to identify molecular and ionic species from spectral features. At 26 GPa water is compressed two-fold and heated to 1700 K. The stimulated Raman scattering from shocked benzene has been measured at 1.2 GPa, indicating the existence of the molecular state at this shock pressure.<sup>40</sup> The emission spectrum of benzene has been measured to 59 GPa to try to identify chemical species in or close to the shock front.<sup>14</sup>

## V. DISCUSSION

Intermolecular repulsion is the dominant effect at high densities and temperatures. The rare gases are the simplest materials to study in this respect, because the physical properties are determined solely by the repulsive potential, provided electronic excitation is negligible. The He Hugoniot data are interpreted only in terms of an effective pair potential, the calculated shock temperatures as large as 20,000 K being much smaller than the ionization potential.<sup>29</sup>

For Ar the upper limit of the "cold" range is a single-shock pressure of 36 GPa, a compression of 2-fold over initial liquid density, and a calculated temperature of 12,000 K. The pair potential derived from Ar shock-wave data is in excellent agreement with pair potentials derived from molecular-beam scattering data, indicating that two-body interactions dominate in the dense fluid. The pair potential derived from Ar shock-wave data has the exponential-six form:<sup>41</sup>

$$\phi(r) = \epsilon \left\{ \left[ \frac{6}{\alpha - 6} \right] \exp [\alpha(1 - r/r^*)] - \left[ \frac{\alpha}{\alpha - 6} \right] \left( \frac{r^*}{r} \right)^6 \right\}, \quad (1)$$

where  $r$  is the intermolecular distance. The Ar Hugoniot data are shown in Fig. 4. Curve D was calculated using only the potential of Eq. (1) and agrees with the data below 36 GPa. At higher pressures the data fall well below Curve D. Agreement with the data is achieved by taking into account electronic excitation and the density dependence of the electron energy gap.<sup>32</sup> A similar result was obtained for Xe.<sup>33</sup> A fundamental conclusion of the rare gas study is that high shock temperature is a very useful probe of the electronic structure at high density and pressure.

The shock-compression data for non-polar molecules can be calculated using the potential of Eq. (1) scaled via corresponding states and by taking into account molecular vibrational and rotational degrees of freedom. The energy parameter  $\epsilon$  is scaled on critical temperature and the distance parameter  $r^*$  on the cube root of critical volume. The procedure is valid systematically to a compression of 2.5 times liquid density for  $N_2$ , CO, Xe,  $O_2$ ,  $CH_4$ , and  $CO_2$ .<sup>41</sup>

The Hugoniot data for liquid  $N_2$ <sup>10,31,42</sup> and CO are shown in Fig. 5.  $N_2$  and CO are isoelectronic, they have virtually identical critical points, and in these experiments they had the same initial density, 0.81 g/cm<sup>3</sup>. Thus, they are expected to have the same Hugoniot curve by the arguments in the preceding paragraph. The curve through the data up to 15 and 30 GPa for CO and  $N_2$ , respectively, was calculated using a potential scaled from Ar via corresponding states<sup>41</sup> and is in excellent agreement with both the  $N_2$  and CO data. This agreement is evidence that  $N_2$  and CO retain their molecular structure up to 30 and 15 GPa, respectively. Deviations from molecular behavior are interpreted as decomposition in both. In the CO case a large number of product molecules are probably formed by chemical reaction. Nitrogen probably undergoes a dissociative phase transition. In fact, double-shock points for nitrogen starting from 20-25 GPa lie above the principal Hugoniot in pressure-volume space. This is the only known material in which this has been observed and is evidence that these points are in a phase transition region. Comparison with theory indicates that the shock temperature is driving the diatomic to monatomic transition in nitrogen at lower pressures than required at room temperature. Above 70 GPa the two Hugoniot curves merge again and atom density appears to dominate over the chemical nature.

Hugoniot data for silica aerogel are shown in Fig. 6. This aerogel is initially 20-fold expanded relative to  $\alpha$ -quartz density. Although the specimens were shock-compressed 6 to 7-fold, the material is still 3-fold expanded relative to crystal density. In an experiment shocked to 6.7 GPa a shock temperature of 10,800 K was measured. Thus, these experiments access a new regime for accurate laboratory measurements on high-temperature expanded-volume states of glass. This material has several important potential uses. It can be a very low shock-impedance equation-of-state standard. It can be used to generate and study few-eV inertially-confined plasmas, as for shocked gases.<sup>43</sup> Its equation of state may be used to understand cratering phenomena because  $SiO_2$  is a major geological material.

Water is a complicated fluid in that the  $H_2O$  molecule is polar and the intermolecular potential is not spherically symmetric. Intermolecular H-bonds have a strong influence on the structure of water, especially at low pressures. The electrical conductivity of shocked water is quite large, about 20 (ohm-cm)<sup>-1</sup> from 30-60 GPa.<sup>17</sup> This conductivity has been interpreted in terms of ionization:  $2 H_2O \rightarrow OH^- + H_3O^+$ . The high conductivity indicates that significant, if not total, ionization does occur.

In order to identify the chemical species in shocked water, spontaneous Raman spectroscopy experiments were performed in the shock pressure range 7.5-26 GPa. Only a broad OH-stretch band is observed at all pressures. A spectrum for 11.7 GPa is shown in Fig. 7. No definite indications of  $OH^-$  or  $H_3O^+$  ions are observed based on the positions of their vibrational bands at ambient. The position of the OH-stretch band is virtually independent of shock pressure and the shape of the OH-stretch band changes in such a way as to indicate the destruction of intermolecular H-bonds, as would be expected. These bonds have a characteristic energy of  $\sim 1000$  K and the shock temperature is about 1,700 K at 26 GPa. The analysis seems to indicate that the  $H_2O$  molecule remains the dominant scattering component with increasing pressure. The  $H_3O^+$  ion is not observed because its presence is associated

with hydrogen-bonded  $\text{H}_2\text{O}$  complexes which are destroyed at these conditions. Absence of  $\text{H}_3\text{O}^+$  means that  $\text{OH}^-$  and  $\text{H}^+$  are most probably the conduction mechanism in strongly shocked water. Evidently, the hydroxyl ion cannot be distinguished from  $\text{H}_2\text{O}$  at high shock pressures.

Chemical decomposition and reaction occurs in shocked hydrocarbons. Benzene, for example, has the distinct volume collapse of a phase transition in its Hugoniot curve at 13 GPa.<sup>44</sup> Optical absorption experiments show that benzene retains its molecular nature up to 13 GPa.<sup>45</sup> The volume collapse at 13 GPa has been interpreted by the formation of dense carbon phases.<sup>34,46</sup> The emission spectra from shock fronts in benzene have been measured in the range 22-59 GPa.<sup>14</sup> A spectrum at 50 GPa is shown in Fig. 8. The spectrum has a broad graybody thermal component with nonequilibrium features superimposed. Features in the spectral range are coincident with the Swann bands for the  $\text{C}_2$  molecule and provide the first spectral evidence for the formation of carbon phases in shocked hydrocarbons.

High dynamic pressure is also used to synthesize new materials. For example, stoichiometric  $\text{Nb}_3\text{Si}$  with a high superconducting transition temperature  $T_c = 18$  K has only been synthesized by processing a nonsuperconducting phase at 100 GPa (1 Mbar) shock pressures.<sup>47</sup> In order to develop the experimental and computational techniques to process materials at 100 GPa shock pressures and recover them for investigations of material structure and physical properties, Nb metal was recently recovered intact from peak dynamic pressures in the range 60-120 GPa.<sup>48</sup> Pressure and effective-plastic-strain histories were calculated using a finite element hydrodynamic computer code. Recovered specimens were characterized by X-ray diffraction, metallography, Vicker's hardness, and  $T_c$ . The maximum change observed in a  $T_c$  of 9.18 K for the unshocked specimen was 0.035 K in the specimen shocked to a maximum pressure of 0.6 Mbar. Shock processing  $\text{V}_3\text{Si}$  at 100 GPa depresses its  $T_c$  by 1.8 K from the initial value of 16.4 K.<sup>49</sup> These results indicate that shock-induced defects and disorder have a relatively weak effect on the  $T_c$  of equilibrium phases and suggest that shock-synthesized metastable superconductors might have  $T_c$ 's close to intrinsic values for the ordered material.

Finally, shock-impedance-match experiments have been performed at ultrahigh pressures using two-stage guns to accelerate impactors to 8 km/s, chemical explosives to drive impactors to 15 km/s, and strong shock waves generated in proximity to underground nuclear explosions.<sup>50-56</sup> At ultrahigh pressures nuclear-explosive-driven experiments are the only ones that provide the required accuracy because of the long shock transit times and steady profile of the shock wave. The Hugoniot data for Cu is summarized in Fig. 9, which is a plot of shock velocity versus mass velocity. The data in this figure span the shock pressure range 0.3-6 TPa (3-60 Mbar). At lower pressures the data fit a linear shock velocity-mass velocity relation, shown as the solid line, which extends up to 1.5 TPa. At higher pressures the data deviates systematically below the extrapolation of the linear fit, which is probably indicative of a transition to Thomas-Fermi behavior at pressures above 10 TPa. The smooth nature of the data are striking considering the variety of techniques that were employed over the  $\sim 25$  years in which this data was accumulated.

#### ACKNOWLEDGEMENT

Work performed under the auspices of the U.S. Department of Energy by the Lawrence Livermore National Laboratory under contract number W-7405-ENG-48.



## REFERENCES

1. "Shock Waves in Condensed Matter-1981," edited by Nellis, W. J., Seaman, L. and Graham, R. A., American Institute of Physics, 1982.
2. "Shock Waves in Condensed Matter-1983," edited by Asay, J. R., Graham, R. A. and Straub, G. K., Elsevier Science Publishers, 1984.
3. Nellis, W. J., "Shocked Fluids at High Densities and Temperatures," in Shock Waves in Condensed Matter-1983, edited by Asay, J. R., Graham, R. A. and Straub, G. K., Elsevier Science Publishers, 1984, p. 31.
4. Taylor, J. W., "Thunder in the Mountains," in Shock Waves in Condensed Matter-1983, edited by Asay, J. R., Graham, R. A. and Straub, G. K., Elsevier Science Publishers, 1984, p. 3.
5. "Shock Waves in Condensed Matter-1981," edited by Nellis, W. J., Seaman, L. and Graham, R. A., American Institute of Physics, 1982, pp. 613-712.
6. Jones, A. H., Isbell, W. M. and Maiden, C. J., "Measurement of the Very-High-Pressure Properties of Materials Using a Light-Gas Gun," *Journal of Applied Physics*, Vol. 37, Aug. 1966, p. 3493.
7. Mitchell, A. C. and Nellis, W. J., "Diagnostic System of the Lawrence Livermore National Laboratory Two-Stage Light-Gas Gun," *Reviews of Scientific Instruments*, Vol. 52, Mar. 1981, p. 347.
8. Mitchell, A. C., Nellis, W. J. and Monahan, B., "Enhanced Performance of a Two-Stage Light-Gas Gun," in "Shock Waves in Condensed Matter-1981," edited by Nellis, W. J., Seaman, L. and Graham, R. A., American Institute of Physics, 1982, p. 184.
9. Nellis, W. J., "Measurements at Ultra-High Dynamic Pressures," in "High Pressure Measurement Techniques," edited by Peggs, G. N., Applied Science Publishers, 1983, p. 69.
10. Nellis, W. J. and Mitchell, A. C., "Shock Compression of Liquid Argon, Nitrogen, and Oxygen to 90 GPa (900 kbar)," *Journal of Chemical Physics*, Vol. 73, Dec. 1980, p. 6137.
11. Nellis, W. J., Ree, F. H., van Thiel, M. and Mitchell, A. C., "Shock Compression of Liquid Carbon Monoxide and Methane to 90 GPa (900 kbar)," *Journal of Chemical Physics*, Vol. 75, Sept. 1981, p. 3055.
12. Lyzenga, G. A. and Ahrens, T. J., "Multiwavelength Optical Pyrometer for Shock Compression Experiments," *Reviews of Scientific Instruments*, Vol. 50, Nov. 1979, p. 1421.
13. Lyzenga, G. A., Ahrens, T. J., Nellis, W. J. and Mitchell, A. C., "The Temperature of Shock-Compressed Water," *Journal of Chemical Physics*, Vol. 76, June 1982, p. 6282.
14. Johnson, M. L., Nicol, M. F. and Holmes, N. C., to be published.
15. Klimenko, V. Y. and Dremine, A. N., "Structure of a Shock Wavefront in a Liquid," in "Detonatsiya," edited by Breusov, O. N., Academy of Sciences of USSR, 1978, p. 79.
16. Hoover, W. G., "Structure of a Shock-Wave Front in a Liquid," *Physical Review Letters*, Vol. 42, June 1979, p. 1531.
17. Mitchell, A. C. and Nellis, W. J., "Equation of State and Electrical Conductivity of Water and Ammonia Shocked to the 100 GPa (1 Mbar) Pressure Range," *Journal of Chemical Physics*, Vol. 76, June 1982, p. 6273.
18. Holmes, N. C., Nellis, W. J., Graham, W. B. and Walrafen, G. E., to be published.
19. Holmes, N. C., Radousky, H. B., Moss, M. J., Nellis, W. J. and Henning, S., "Silica at Ultrahigh Temperature and Expanded Volume," *Applied Physics Letters*, Vol. 45, Sept. 1984, p. 626.
20. Trainor, R. J., Shaner, J. W., Auerbach, J. M. and Holmes, N. C., "Ultrahigh-Pressure Laser-Driven Shock-Wave Experiments in Aluminum," *Physical Review Letters*, Vol. 42, April 1979, p. 1154.

21. Barker, L. M. and Hollenbach, R. E., "Interferometer for Measuring High Velocities of Any Reflecting Surface," *Journal of Applied Physics*, Vol. 43, Nov. 1972, p. 4669.
22. Durand, M., Laharrague, P., Lalle, P., Le Bihan, A., Morvan, J. and Pujols, H., "Interferometric Laser Technique for Accurate Velocity Measurement in Shock Wave Physics," *Reviews of Scientific Instruments*, Vol. 48, March 1977, p. 275.
23. Barker, L. M., "High-Pressure Quasi-Isentropic Impact Experiments," in "Shock Waves in Condensed Matter-1983," edited by Asay, J. R., Graham, R. A. and Straub, G. K., Elsevier Science Publishers, 1984, p. 217.
24. McQueen, R. G., Hopson, J. W. and Fritz, J. N., "Optical Technique for Determining Rarefaction Wave Velocities at Very High Pressures," *Reviews of Scientific Instruments*, Vol. 53, Feb. 1982, p. 245; Brown, J. M. and McQueen, R. G., "Melting of Iron Under Core Conditions," *Geophysical Research Letters*, Vol. 7, July 1980, p. 533.
25. Radousky, H. B., Ross, M., Mitchell, A. C. and Nellis, W. J., "Shock Temperatures and Melting in CsI," *Physical Review B*, Vol. 31, Feb. 1985, p. 1457.
26. Johnson, Q., Mitchell, A. C. and Smith, I. D., "Flash X-ray Tube for Diffraction Studies on a Two-Stage Light-Gas Gun," *Reviews of Scientific Instruments*, Vol. 51, June 1980, p. 741.
27. Johnson, Q. and Mitchell, A. C., "Flash X-ray Diffraction Studies to 100 GPa," in "High Pressure Science and Technology," Vol. 2, edited by Vodar, B. and Marteau, Ph., Pergamon, 1980, p. 977.
28. Nellis, W. J., Mitchell, A. C., van Thiel, M., Devine, G. J., Trainor, R. J. and N. Brown, "Equation-of-State Data for Molecular Hydrogen and Deuterium at Shock Pressures in the Range 2-76 GPa (20-760 kbar)," *Journal of Chemical Physics*, Vol. 79, Aug. 1983, p. 1480.
29. Nellis, W. J., Holmes, N. C., Mitchell, A. C., Trainor, R. J., Governo, G. K., Ross, M. and Young, D. A., "Shock Compression of Liquid Helium to 56 GPa (560 kbar)," *Physical Review Letters*, Vol. 53, Sept. 1984, p. 1248.
30. Johnson, J. D., Shaw, M. S. and Holian, B. L., "The Thermodynamics of Dense Fluid Nitrogen by Molecular Dynamics," *Journal of Chemical Physics*, Vol. 80, Feb. 1984, p. 1279.
31. Nellis, W. J., Holmes, N. C., Mitchell, A. C. and van Thiel, M., "Phase Transition in Fluid Nitrogen at High Densities and Temperatures," *Physical Review Letters*, Vol. 53, Oct. 1984, p. 1661.
32. Ross, M., Nellis, W. and Mitchell, A., "Shock-Wave Compression of Liquid Argon to 910 kbars," *Chemical Physics Letters*, Vol. 68, Dec. 1979, p. 532.
33. Nellis, W. J., van Thiel, M. and Mitchell, A. C., "Shock Compression of Liquid Xenon to 130 GPa (1.3 Mbar)," *Physical Review Letters*, Vol. 48, March 1982, p. 816.
34. Nellis, W. J., Ree, F. H., Trainor, R. J., Mitchell, A. C. and Boslough, M. B., "Equation of State and Optical Luminosity of Benzene, Polybutene, and Polyethylene Shocked to 210 GPa (2.1 Mbar)," *Journal of Chemical Physics*, Vol. 80, March 1984, p. 2789.
35. Radousky, H. B., Mitchell, A. C. and Nellis, W. J., to be published.
36. Voskoboinikov, I. M., Gogulya, M. F. and Dolgoborodov, Yu. A., "Temperatures of Shock Compression of Liquid Nitrogen and Argon," *Soviet Physics Doklady*, Vol. 24, May 1979, p. 375.
37. Hamann, S. D., "Properties of Electrolyte Solutions at High Pressure," in "Modern Aspects of Electrochemistry," No. 9, edited by Conway, B. E. and Bockris, J. O'M., Plenum, 1974, p. 126.
38. Kovel, M. I., "The Shock Wave Hugoniot and Electrical Conductivity of Liquid Ammonia in the Pressure Range 45-282 kbar," Lawrence Livermore National Laboratory Report UCRL-51367, March, 1973.

39. Hamilton, D., Mitchell, A. C., and Nellis, W. J., to be published.
40. Schmidt, S. C., Moore, D. S., Schiferl, D. and Shaner, J. W., "Backward Stimulated Raman Scattering in Shock-Compressed Benzene," *Physical Review Letters*, Vol. 50, Feb. 1983, p. 661.
41. Ross, M. and Ree, F. H., "Repulsive Forces of Simple Molecules and Mixtures at High Density and Temperature," *Journal of Chemical Physics*, Vol. 73, Dec. 1980, p. 6146.
42. Zubarev, V. N. and Telegin, G. S., "The Impact Compressibility of Liquid Nitrogen and Solid Carbon Dioxide," *Soviet Physics Doklady*, Vol. 7, July 1962, p. 34.
43. Fortov, V. E., "Shock-Wave Production of a Non-Ideal Plasma," *Soviet Physics JETP*, Vol. 44, July 1976, p. 116.
44. Dick, R. D., "Shock Wave Compression of Benzene, Carbon Disulfide, Carbon Tetrachloride, and Liquid Nitrogen," *Journal of Chemical Physics*, Vol. 52, June 1970, p. 6021.
45. Yakusheva, O. B., Yakushev, V. V. and Dremin, A. N., "The Opacity Mechanism of Shock-Compressed Organic Liquids," *High Temperatures-High Pressures*, Vol. 3, 1971, p. 261.
46. Yakusheva, O. B., Yakushev, V. V. and Dremin, A. N., "Relation Between Loss of Transparency by Carbon Compounds under High Dynamic Pressures and Anomalies on the Impact Compressibility Curves," *Russian Journal of Physical Chemistry*, Vol. 51, 1977, p. 973.
47. B. Olinger and L. R. Newkirk, "Bulk Al<sub>5</sub>, High T<sub>c</sub> Nb<sub>3</sub>Si Synthesized by Shock Compression," *Solid State Communications*, Vol. 37, Aug. 1981, p. 613.
48. Nellis, W. J., Moss, W. C., Radousky, H. B., Mitchell, A. C., Summers, L. T., Dalder, E. N., Maple, M. B. and McElfresh, M., "Superconducting Critical Temperatures of Niobium Recovered from Megabar Dynamic Pressures," *Lawrence Livermore National Laboratory Report UCRL-92742*, June, 1985.
49. Stewart, G. R., Olinger, B. and Newkirk, L. R., "Degradation of Superconductivity in Al<sub>5</sub> V<sub>3</sub>Si by Explosive Compression," *Physical Review B*, Vol. 31, March 1985, p. 2704.
50. Altshuler, L. V., Kormer, S. B., Bakanova, A. A., and Trunin, R. F., "Equation of State for Aluminum, Copper, and Lead in the High Pressure Region," *Soviet Physics JETP*, Vol. 11, Sept. 1960, p. 573.
51. Altshuler, L. V., Bakanova, A. A. and Trunin, R. F., "Shock Adiabats and Zero Isotherms of Seven Metals at High Pressures," *Soviet Physics JETP*, Vol. 15, July 1962, p. 65.
52. Trunin, R. F., Podurets, M. A., Moiseev, B. N., Simakov, G. V. and Popov, L. V., "Relative Compressibility of Copper, Cadmium, and Lead at High Pressures," *Soviet Physics JETP*, Vol. 29, Oct. 1969, p. 630.
53. Trunin, R. F., Podurets, M. A., Simakov, G. V., Popov, L. V. and Moiseev, B. N., "An Experimental Verification of the Thomas-Fermi Model for Metals Under High Pressure," *Soviet Physics JETP*, Vol. 35, Sept. 1972, p. 550.
54. Mitchell, A. C. and Nellis, W. J., "Shock Compression of Aluminum, Copper, and Tantalum," *Journal of Applied Physics*, Vol. 52, May 1981, p. 3363.
55. Ragan, C. E., "Shock-Wave Experiments at Threefold Compression," *Physical Review A*, Vol. 29, March 1984, p. 1391.
56. Mitchell, A. C., Nellis, W. J., Heinle, R. A., Repp, G. W., Moriarty, J. A., Ross, M. and Holmes, N. C., to be published.

Table 1. Summary of shock-compression experiments for fluids.  $T_0$  is initial temperature,  $\rho_0$  is initial density,  $\rho_{\max}$  is maximum density, and  $P_{\max}$  is maximum shock pressure.

Liquid	$T_0$ (K)	$\rho_0$ (g/cm <sup>3</sup> )	$\rho_{\max}$ (g/cm <sup>3</sup> )	$P_{\max}$ (GPa) <sup>a</sup>
Helium	4	0.12	0.68	56
Deuterium	20	0.17	0.96	76
Hydrogen	20	0.07	0.23	10
Nitrogen	77	0.81	2.8	82
Oxygen	77	1.2	3.3	86
Carbon Monoxide	77	0.81	3.0	69
Methane	111	0.42	1.6	92
Benzene	295	0.89	2.4	70
Polybutene	295	0.89	2.7	210
Argon	87	1.4	3.8	91
Xenon	165	3.0	9.6	130
Ammonia	230	0.69	1.8	64
Water	295	1.0	3.5	220

<sup>a</sup>1 GPa = 10 kbar.

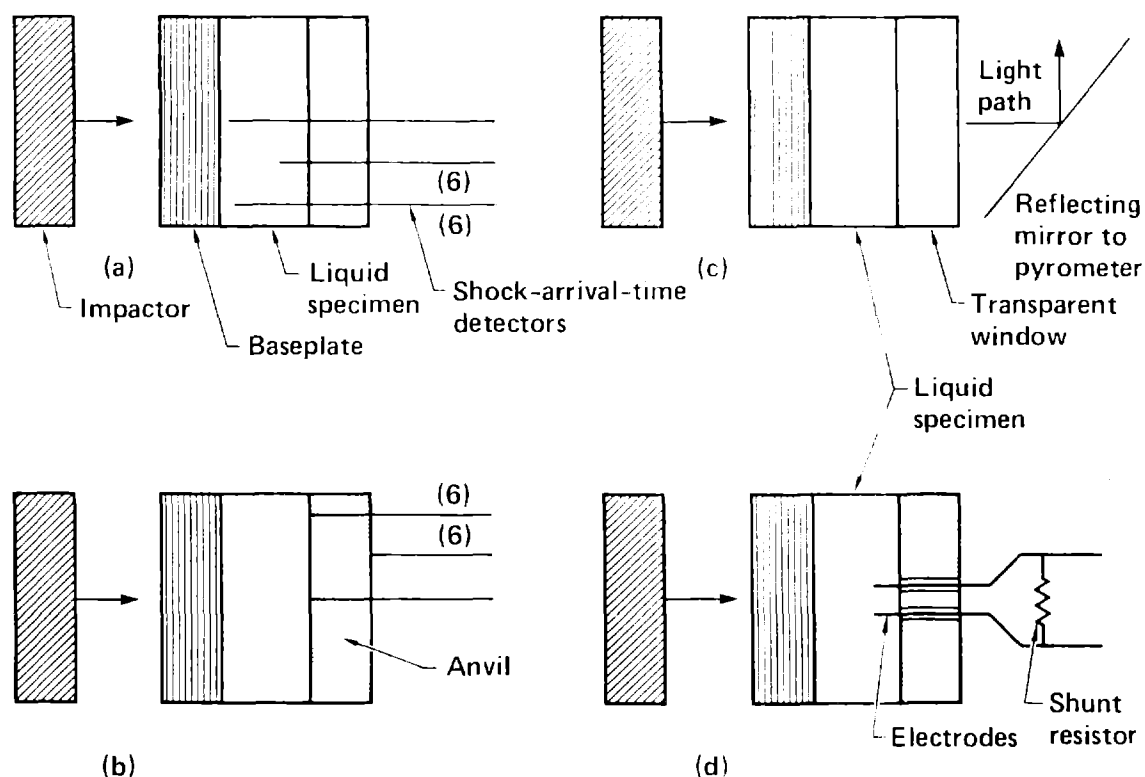


Figure 1. a) Schematic of single-shock equation-of-state experiment.<sup>10</sup> b) Double-shock equation-of-state experiment.<sup>11</sup> c) Shock temperature<sup>13</sup> or emission spectroscopy<sup>14</sup> for transparent liquid specimen. d) Electrical conductivity experiment.<sup>17</sup>

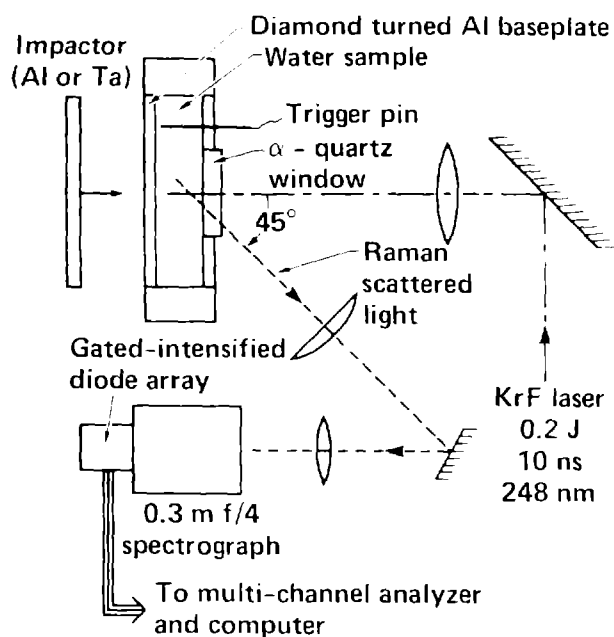


Figure 2. Schematic of pulsed, spontaneous, Raman scattering experiment in shocked water.<sup>18</sup>

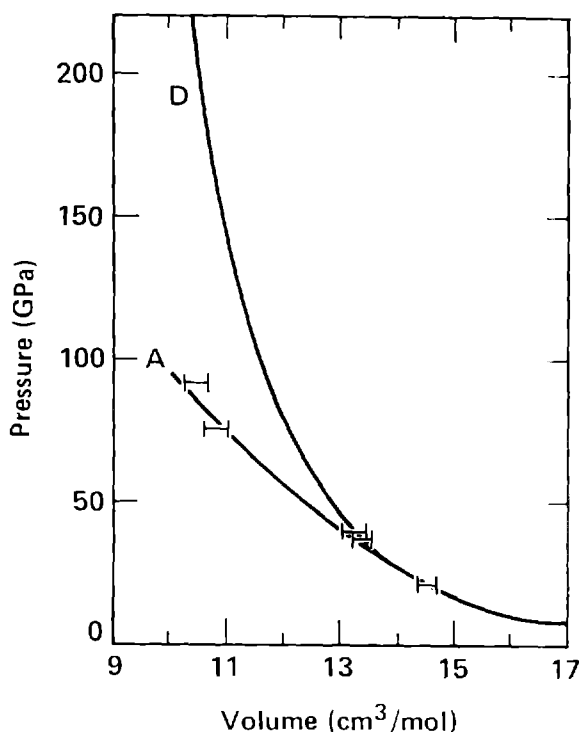


Figure 4. Hugoniot data for shocked liquid Ar.<sup>10</sup> Curve A was calculated taking into account interatomic repulsion and electronic excitation across volume-dependent electron energy gap. Curve D was calculated neglecting electronic excitation.<sup>32</sup>

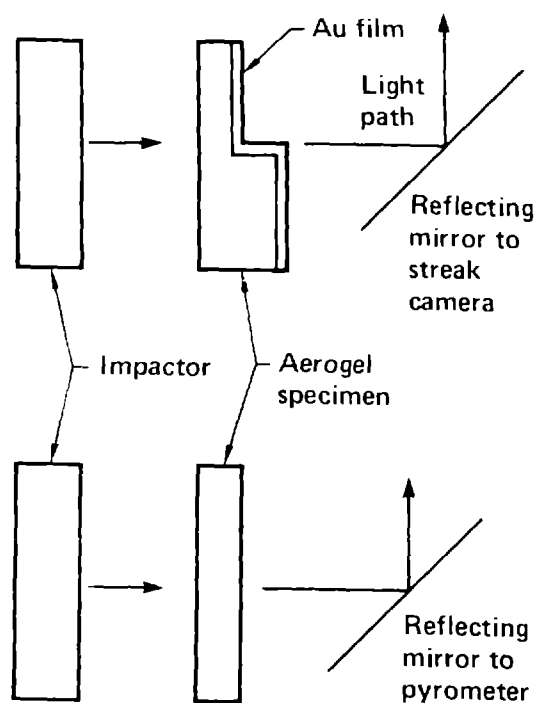


Figure 3. Schematic of equation-of-state (top) and shock temperature (bottom) experiments for shocked transparent silica aerogel. At top, Au coating screens thermal radiation from a streaking camera until shockwave reaches rear surfaces of stepped target. At bottom, light emitted from the shock front is sent to a pyrometer during transit time of shock through specimen.<sup>19</sup>

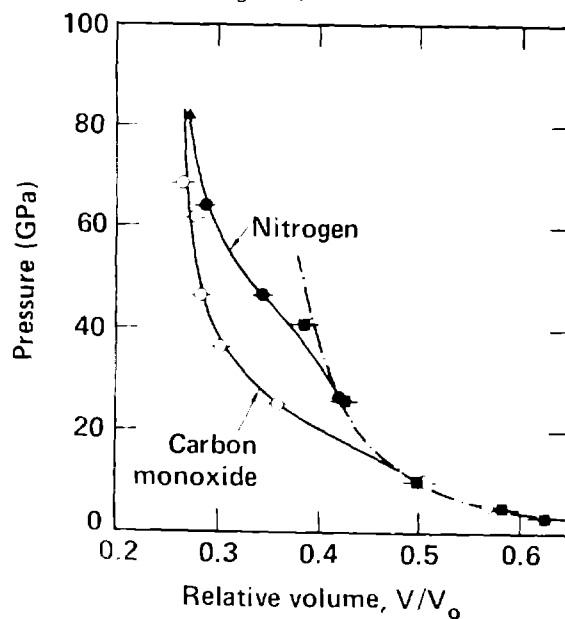


Figure 5. Hugoniot data for shocked liquid N<sub>2</sub><sup>10,31,42</sup> and isoelectronic CO.<sup>11</sup> Dash-dot curve is theory<sup>41</sup> for both molecular N<sub>2</sub> and CO. Initial volume of both is 34.7 cm<sup>3</sup>/mole.

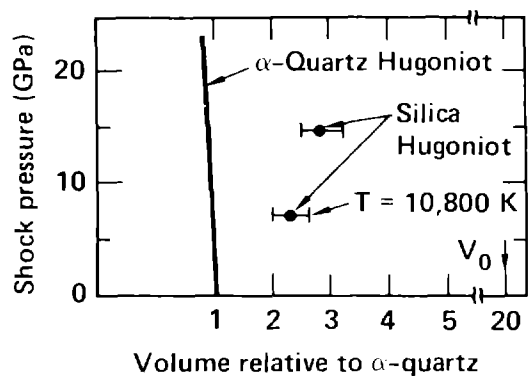


Figure 6. Hugoniot data for silica aerogel, which is porous  $\text{SiO}_2$  expanded 20-fold relative to  $\alpha$ -quartz density.<sup>19</sup> Although aerogel is compressed substantially, the final densities are still less than crystal density. Indicated temperature was measured pyrometrically.

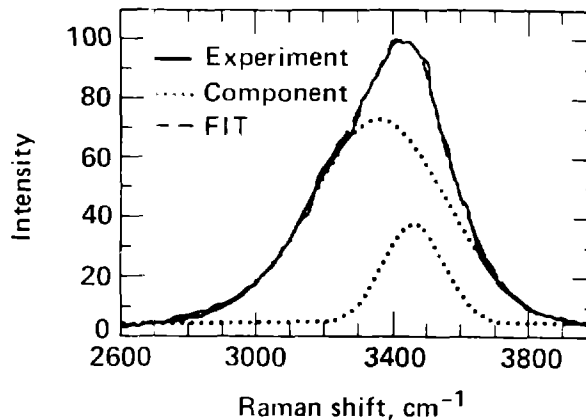


Figure 7. Spontaneous Raman spectrum from water shocked to 11.7 GPa<sup>18</sup> using system in Fig. 2. Spectrum is sum of two gaussian components shown.

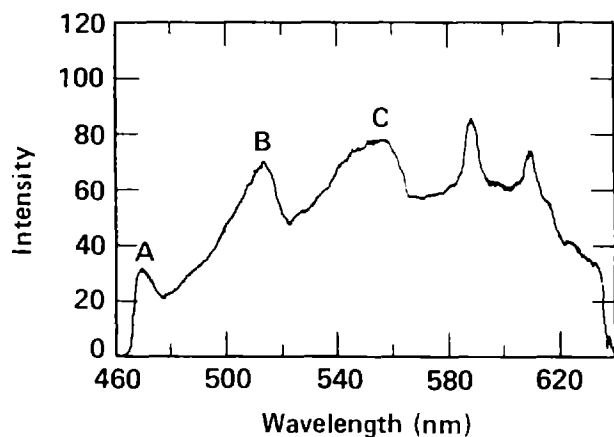


Figure 8. Emission spectrum from benzene shocked to 50 GPa.<sup>14</sup> Features labelled A, B, C are coincident with the Swann bands for  $\text{C}_2$  molecule.

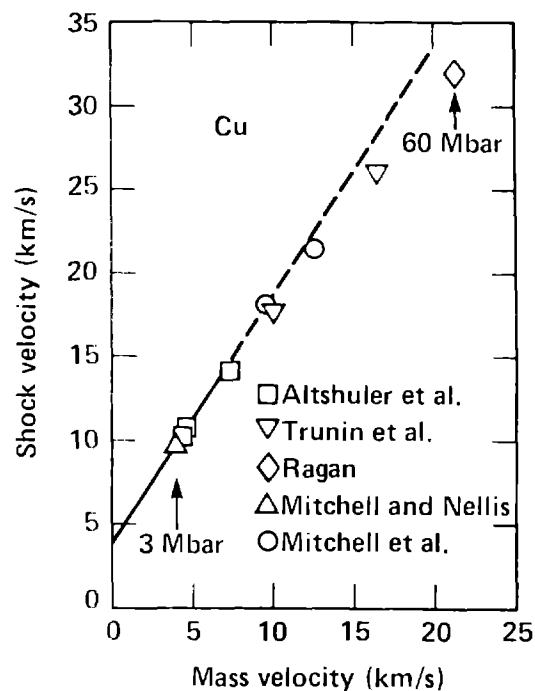


Figure 9. Shock velocity versus mass velocity for Cu spanning range 0.3-6 TPa (3-60 Mbar).<sup>50-56</sup>